Paper# 2001-0351

Flow Control with Electrohydrodynamic Actuators

Guillermo Artana*, Juan D'Adamo†, Luc Léger‡, Eric Moreau§, Gérard Touchard¶

ABSTRACT

This work analyses the ability of an electrohydrodynamic actuator to modify the characteristics of a flow over a flat plate. The device considered uses flush mounted electrodes and a d.c. power supply to create a plasma sheet on the surface of the plate. We analyze the mechanism of formation of this plasma sheet, which is shown to be similar to the streamer formation. We show flow visualizations at low flow velocities (≈1m/s) and results from Particle Image Velocimetry at higher flow velocities (range 11.0-17.5 m/s). These results show that the discharge can induce an important acceleration of the flow close to the surface.

INTRODUCTION

Coronas are self sustaining discharges characterized by a strong inhomogeneity of the electric field configuration and electrodes having a low curvature radius. This configuration confines the ionization process to regions close to the high-field electrodes. Thus, in this phenomena there are active electrodes, surrounded by ionization regions where free charges are created, a low-field drift region where charged particles drift and react and low-field passive electrodes.

Coronas can be unipolar or bipolar if one or both electrodes are active electrodes. Bipolar coronas can lead to the formation of streamers, a weakly conducting plasma filament extending from one electrode and carrying its own ionization region ahead of itself. Positive streamers are cathode-directed and negative streamers anode-directed.

The knowledge of the physics of corona discharge occurring in a gas close to an insulating surface has not been as widely studied as has occurred with coronas without any extraneous bodies in the vicinity of the discharge [1-2].

As the discharge involves the movement of ions but also a large amount of neutral particles, this situation becomes of special interest in aerodynamics for flow and instabilities control.

The induced fluid motion is usually called electroconvection and sometimes electric wind. Coulombian electroconvection takes place if the coulombian forces acting on the fluid particles are predominant in relation to the polarization ones. This is usually the case when the fluid medium is air. The way the electric forces act on fluid particles may be explained by considering that ions in their drift motion from one electrode to the other, will exchange momentum with the neutral fluid particles and induce their movement.

As currents involved in the process are so low that magnetic effects can be disregarded the phenomena is described by the set of equations used in electrohydrodynamics (EHD) problems.

In the present work, actuators based on electroconvection will be called electrohydrodynamic actuators. Main advantages of these actuators are that they have no moving part and a very short response time (delays are of the order of nanoseconds)

If the discharge takes place quite close to a surface the velocity field close to this region can be greatly modified. So, in wall bounded or wake flows configurations, electroconvection is a good candidate to control the transition of boundary layers from laminar to turbulent types, to change the position of the separation line, or to modify the stability of coherent structures.

A large part of prior research of electrohydrodynamic actuators in air has been concerned with the possibility of heat transfer augmentation [3-7] and of drag reduction [8-14] . Also, some works have analyzed the effects of the electroconvection on the special flow configuration appearing in some industrial process like those in an electrostatic precipitator [15-17].

*Professor, Department of Mechanical Engineering, Faculty of Engineering, University of Buenos Aires, CONICET, Buenos Aires, Argentine.
†Tutor, Department of Mechanical Engineering, Faculty of Engineering, University of Buenos Aires, Buenos Aires, Argentine.
‡Ph. D. Student, Laboratoire d'Etudes Aerodynamiques (UMR 6609 CNRS), University of Poitiers, Poitiers, France
§Maitre de Conferences, Laboratoire d'Etudes Aerodynamiques (UMR 6609 CNRS), University of Poitiers, Poitiers, France
¶Professor, Laboratoire d'Etudes Aerodynamiques (UMR 6609 CNRS), University of Poitiers, Poitiers, France

The effects of the ionization of the gas upstream of a shock wave, and the possibility of using it to control the flow over hypersonic vehicles has been receiving special attention [18-21].

Though these research works show that injected ions can modify the characteristics and stability of the main flow, these devices (like most of the actuators currently considered in active fluid mechanic research) need substantial development.

With a few exceptions[10-12], most of the research has been undertaken with electrodes placed at some distance form the wall with an increase of momentum mainly in the direction of the normal to the surface.

If the electrodes were placed flush-mounted on the wall surface and momentum added to the fluid tangentially to the wall we think that it should be more effective to achieve better devices to control some characteristics of the flows (like the skin friction forces, heat transfer, ...).

On this principle, some electrohydrodynamic devices based on a surface generated atmospheric radio frequency (RF) plasma have been proposed.

The device named one atmosphere uniform glow discharge (OAUGDP) uses two electrodes separated by an insulating surface that avoids the knocking of the ions on the cathode preventing the heating of it and the formation of new avalanches or breakdown from electron secondary emission[22]. The authors claim that paraelectric forces associated to electric field gradients enable ion acceleration and via particle collision acceleration of the neutral particles. Other devices like the OAUGDP but with a polyphase RF power have been presented recently [23-24].

The present work proposes a different approach as we use both electrodes flush mounted on an insulating surface and we consider a bipolar corona obtained with a d.c. discharge.

Recent results[25,26], indicate that with this electrode configuration in insulating cylinders, some aspects of the discharge are similar to the coronas behavior. In these article is shown that under some circumstances a special regime can be observed: it is similar to a glow discharge as the drift region of the "normal" coronas almost fully disappears.

From a technological point of view, the use of this configuration has advantages like simplicity, and because of its uniformity a high efficiency to transform electrical into mechanical power.

However, in view of achieving a reliable device is still necessary to get a better knowledge of the characteristic of the discharge under different conditions to operate it with a higher control degree.

The target of this work is to analyze the discharge characteristics produced by electrodes flush mounted on a surface of a flat plate and how the electroconvection they produce modifies the fluid mechanics occurring around the plate when traversed by an air flow.

EXPERIMENTAL SETUP

In our study the injection of ions is obtained with a d.c. corona discharge between a wire type electrode (0.90 mm diameter) and a plane electrode of aluminum foil (of the same length than the wire).

The electrodes are located flush mounted on the surface of a flat plate of PMMA (5mm thick) as shown in Figure 1.

Two different H.V. sources of opposite polarity (+20kV, -20kV, 1.5 mA) impose a voltage difference between both electrodes.

The wire type electrode is connected to the positive polarity source and the plate electrode to the negative one. By increasing the voltage difference between both electrodes different discharge regimes can be established. The current measurement is undertaken with an electrometric circuit which can detect currents of 1 nA. The characteristic voltage current curves are determined using the setup indicated in Figure 2.

A plate similar to that but shorter, has been placed horizontally and parallel to the main flow in a wind tunnel (0-5 m/s, 0.28 x 0.28 m^2 rectangular cross section, turbulence level lower than 3%). The wire electrode was facing the flow in the frontal stagnation point. A schematic of the wind tunnel is shown in Figure 3. Velocity measurements of the flow were taken with a micromanometer (accuracy 0.04Pa) and a pitot probe.

Visualizations at low velocities have been done using a laser sheet produced by a 5W argon-ion laser and a single smoke filament (ϕ=2mm). Seeding was produced with a smoke generator EI 514 Deltalab that uses a pure cosmetic grade oil and operated to obtain a cloud with a mean particle diameter of 0.3μm. Images are recorded with a videocamera and then digitalized.

Particle image velocimetry (PIV) measurements have been done in a closed wind tunnel with a probe section of 0.50x0.50m^2 and a range of velocities of 2-30m/s.

The experiments have been conducted using the DANTEC system controlled by FlowMap® PIV. Interrogation area was 32 × 32 pixels with an overlap of 50 % . Seeding was also done with particles of a pure cosmetic grade oil like in the visualization experiments and with the same mean diameter.

The system was illuminated with a laser sheet produced by a Yag laser of 200mJ. In our experiments each pulse had a duration of 0.01 microseconds and the time between a pair of pulses was 50 microseconds.

The progressive scan interline camera we used can produce images of 768 × 484 pixels. We considered 600 pairs of digital images taken every 0.1 seconds to obtain the velocity field of the airflow.

EXPERIMENTAL RESULTS

Discharge Characteristics

The characteristics of the different discharge regimes in our case are described here below and a typical voltage-current curve is shown in Figure 4. The different regimes are quite similar to the ones occurring in a cylindrical geometry with electrodes flush mounted described in a previous work[25].

Spot type regime: The discharge is concentrated in some visible spots of the wire and by increasing the voltage difference they can increase in number. Some of them may ionize in a plume-like type or may lead to a narrow channel quite attached to the surface. In Figure 4 this regime corresponds to the range of currents lower than 0.2 mA/m

Generalized glow regime: At higher voltage differences, a regime characterized by a homogeneous luminescence can be observed. This luminescence occupies the whole interelectrode space almost all along the wire. The discharge makes the plate surface appear to look like supporting a thin film of ionized air. This discharge is quite homogeneous noisy and the current quite stable with time. By visual inspection it appears that the thickness of the ionized film is of the order of the thickness of the aluminum foil (50 micrometers). Measurements with a multiplier photometer indicate an intensity of the luminosity of the discharge close to 0.5 microlumen.
In Figure 4 this regime corresponds to currents between 0.2-0.8mA/m. The discharge is largely dependent on the quality of the finishing of the electrodes. Sometimes it is hard to start and it can be promoted by blowing towards the plate surface hot air like the one produced with a hair drier. In the range of velocities of our experiments (0.5-20m/s) the intensity of the current of the discharge was not significantly modified by a flow of air.

Filament type regime: In this regime some points of the wire have a concentrated discharge in an arborescent shape or in filament type. By further increasing the voltage some localized sparks appear following a non-rectilinear trajectory at small distance from the surface.

In the present work we have undertaken the flow measurements in the generalized glow regime.

Flow Visualisation

Figures 5a and b are photos which show typical visualizations at low velocity ranges (V≈1m/s). They show the changes on the smoke tracers filaments when the discharge is applied (wire electrode is upstream).

PIV data processing

Each velocity field is filtered with a peak-validation and a range validation filter. Peak validation filter is based on the detectability criterion[27] which validates vectors with a ratio of the highest peak to the second highest peak in the correlation plane larger than a fixed value (1.2 in our case). The range validation filter enables to establish the range admitted for the modulus of the velocity vectors. In our case we have considered a value of 2.0 times the flow velocity Uo as the upper limit. Undertaking these filtering processes, about 50 to 100 vectors are removed from 1363 initial vectors.

An average on 600 vector fields is performed in order to obtain a mean velocity field of the airflow in one experiment. We show results concerning to this mean velocity field in Figures 6 a, b and c. These figures show at different flow velocities (11.0, 14.0 and 17.5m/s) the difference of these averaged vectors for the cases with discharge on and discharge off.

DISCUSSION

Physical interpretation of the electrical results

In the last twenty years different researchers[28-34] were interested by a discharge in a configuration with some similarities with the one we consider here. Their goal was to obtain a uniform high current surface discharge at moderate voltages for gas-lasers use.

The device considered was similar to the one we used. It consisted on electrodes flush mounted on the surface of a dielectric plate but they were excited with a pulsed voltage difference. Also in the reverse side of the plate a grounded electrode was placed.

The different discharge regimes for this pulsed discharge were described by Baranov et al[31,34]. They are quite similar to the ones we have observed with our d.c. excitation.

They have also observed that at a certain range of voltages and depending on specific conditions of the experiments, a uniform luminosity like a plasma sheet covering the space between both electrodes takes place. This phenomena has been reported with different names like sliding discharge, grazing discharge or skimming discharge.

Rutkevich[33,34] proposed a model of a stationary wave of ionization to describe the propagation of this discharge. He considered as boundary conditions a perfect dielectric solid with only polarization charges. Ion deposition and surface conduction were neglected.

In this model the transverse component of the electric field near the dielectric surface plays an important role in the development of impact ionization. The non-uniformity of the impact

ionization frequency in that direction is the main reason for forming the plasma sheet.

With this model different parameters can be estimated (velocity of propagation, ion density, ...) and an estimation of the thickness of the plasma sheet Δ is proposed as:

$$\Delta = \frac{1}{\lambda_e} \ln\left(\frac{n_{ew}}{n_0}\right) \qquad (1)$$

with λ_e the inverse of the thickness of the boundary layer for concentrations of electrons near the wall, n_{ew} the concentration of electrons in the gas immediately adjoining the wall and n_0 a value that oscillates between 10^{12} and 10^{14} m^{-3}.

Typical results of the plasma sheet obtained with this model oscillate between 0.1-1mm, apparently of the same order of the one we observed.

The similarities that exists between both processes, the pulsed voltage case and the d.c. voltage case, indicate that the discharge with a d.c. power should, like in a point-to-plane repetitive streamer, be a pulsating discharge.

The scheme would be a repetition of ionization waves, each front of ionization screening the electric field and impeding the formation of a new discharge until the neutralization of the effect of the front.

The initiation of the plasma sheet by the use of hot air seems also to be associated, like in point to plane repetitive streamers, with the creation of lower density air channels [35].

This seems to be the more plausible mechanism to explain the formation of the plasma sheet with a d.c. power but further experiments and the use of a refined model including surface conduction and charge deposition-removal from the surface are still needed to fully describe the phenomena.

A rough analysis of the voltage-current curve can be undertaken if we use as in other works[10-11] the semiempirical approach proposed by Seaver [36]. There, the voltage-current characteristics are given by

$$I_c = \frac{kT}{\chi_i q R}\left(e^{\chi_i q(\Delta\phi-\phi_0)/kT} - 1\right) \qquad (A/m) \qquad (2)$$

with Ic the current per unit length of electrode, $\Delta\phi$ the potential difference between the two electrodes, k is the Boltzmann constant, T is the absolute temperature, q is the ion charge, χ_i is a ratio known as the ion-to-neutral excess momentum concentration, R is a constant representing the gas phase resistance outside the corona wire units (m^{-1} Ω). ϕ_0 is a constant associated with the voltage breakdown that can be estimated with

$$\phi_0 = E_c a \ln(S/a) \qquad (V) \qquad (3)$$

with E_c the corona onset voltage (roughly in our case $\approx 10^6$-10^7V/m), S the electrode spacing and a the curvature radius of the electrode.

The fitting of our results with this function and least square methods gives the following adjusted parameters

Φ_0=0.526 kV

R=35.0 kΩ/m

$$\frac{q\chi_i}{kT} = 0.148 \text{ kV}^{-1}$$

These values are similar to those obtained by Colver[10-11] and the corresponding breakdown field in our case is Ec=2.7 10^6 V/m.

Finally, from our experiments it can be observed that typical values of power consumption per unit area associated with the plasma sheet are about 500W/m^2. They are of the same order than those needed to sustain a glow discharge with the OGADUP device.

Fluid mechanics results interpretation

In flow visualisation by smoke injection techniques or PIV experiments, the trajectories of the seeding particles and those of the surrounding fluid particles are usually considered the same.

This occurs when the seeding particle follows closely the surrounding fluid particles. When there is a slipping velocity $V=U_p-U_f$ the trajectories may differ.

Though particle motion in a moving fluid is a rather complicated phenomena, Hinze's model[37] is usually accepted to describe (at least "qualitatively") the motion of the seeding particles used in PIV experiments. The model gives an expression that enables to establish the limits of the particle size to track properly the flow. It expresses the following balance of forces

$$\frac{\pi}{6} d_p^3 \rho_p \frac{d\hat{U}_p}{dt} = F_{st} + F_p + F_f + F_u \qquad (4)$$

where d_p means diameter of the particle, U velocity, ρ density and subscript p refer to particle and subscript f to fluid. Forces in the right side of equation are defined as

$$F_{st} = -3\pi\mu d_p \hat{V}$$

$$F_p = \frac{\pi}{6} d_p^3 \rho_f \frac{d\hat{U}_f}{dt}$$

$$F_f = -\frac{\pi}{12} d_p^3 \rho_f \frac{d\hat{V}}{dt}$$

$$F_u = -\frac{3}{2} d_p^2 \sqrt{\pi\mu\rho_f} \int_{to}^{t} \frac{d\hat{V}}{d\zeta} \frac{d\zeta}{\sqrt{t-\zeta}}$$

where μ is the coefficient of dynamic viscosity. F_{st} describe the viscous drag as given by Stokes law, F_p is the pressure gradient force, F_f takes into account the resistance of an inviscid fluid to acceleration of the seeding particle and F_u is the Basset history integral that represent the drag force associated with unsteady motion.

The formula is valid under different assumptions (low particle density, particles are spherical,...) but one of the strongest in our case is that the electrostatic forces are negligible. As some smoke particles can be charged by ion impact, coulombian forces would act on them affecting tracer trajectory. So, electrostatic forces should be added in our case to the left side of Hinze equation.

To evaluate the magnitude of the electrostatic forces we consider Bailey's work[38]. He indicates that when a particle is subjected to field directed fluxes of positive and negative ions, both charging and neutralization processes occur simultaneously.

Nevertheless, a net charge develops which depends upon the difference in the rate at which the two flux types are intercepted.

These rates are functions of the ion mobility and of the ionic density of each ion type. When a particle achieves a net charge level the rate at which it receives charge of different signs is the same.

The maximum net charge level q_n which is attained after an exposure time of a few time constants is given by[38]

$$q_n = \pi d_p^2 \varepsilon_0 E_0 \left[\frac{2(\varepsilon_r - 1)}{\varepsilon_r + 2} + 1 \right] \frac{1 - \left(N_- \mu_- / N_+ \mu_+ \right)^{1/2}}{1 + \left(N_- \mu_- / N_+ \mu_+ \right)^{1/2}} \quad (5)$$

with ε_0 Faraday constant, N_+ and N_- the density of positive and negative ions, and μ_+ and μ_- their respective mobilities. An upper limit of the attainable charge for droplets of non polar hydrocarbon (relative dielectric constant $\varepsilon_r \approx 2$) is obtained with

$$q_n \approx 1.5 \pi d_p^2 \varepsilon_0 E_0 \quad (6)$$

Considering this limit it is seen that coulombian forces are proportional to the surface of the particle and to the square of the electric field E_0.

As the influence of the electric forces is less important when the seeding particle diameter is very low, an inspection of Equation (4) corrected with the electrostatic forces, shows that these last forces will be important only when the slipping velocity is very low. For instance considering a particle in air of $d_p = 1\mu m$ and an electric field of $\approx 10^6$V/m, the ratio of the viscous to the electric forces is

$$\frac{F_{st}}{F_{el}} = -\frac{3\pi\mu d_p}{q_m \hat{E}_0} \hat{V} \approx 4.066\,(s/m)\hat{V} \quad (7)$$

where we see that the ratio is directly dependent on the slipping velocity V and that Stokes forces are much larger than electric ones except for low values of V.

In conclusion, for visualization and PIV analysis the seeding particles should be chosen as large as possible in order to scatter most of the light. However, the largest size is limited for the reasons given above to particles of about 1μm when a non polar hydrocarbon is the seeding material. Considering the data sheet given by the constructor of the smoke generator, in our experiments the seeding particles we have used are in the range of 0.3μm. So, in our PIV and visualization experiments the influence of coulombian forces on tracers trajectory in a first approach can be disregarded.

Flow visualization

Flow visualization by smoke injection technique gives an idea of the changes in the flow field that the discharge produces. In these experiments we considered low flow velocities ($U_0 \approx 1$m/s)

Figures 5 shows results at 0.8m/s flow velocities with the discharge operating in the generalized glow regime.

We observe there that the filaments of the smoke tracers tend to approach to the plate when the discharge is applied.

This indicates a tangential acceleration of the air close to the surface of the plate, creating a depression that tends to make the streamlines approach the surface.

This intense effect is greatly reduced if the discharge operates in other regime (spot or filament type). There the 2-D character of the flow is lost and the coincidence of the discharge channels with the region of interest (the plane of visualization) is sometimes difficult.

Particle Image velocimetry

We considered larger flow velocities in our PIV experiments. The results were obtained at flow velocities of 11.0-14.0 and 17.5 m/s and though corresponding to a very different range from those of flow visualization they are in good agreement.

We observe in Figures 6 a, b and c, a relatively important acceleration of the fluid close to the plate surface when compared to the flow velocity.

The comparison of these figures show that, the velocity differences produced by the EHD actuator in the region close to the wall are more important as flow velocities increases. The maximum values detected of the differences are 4.6, 4.9 and 10.7 m/s corresponding respectively to flow velocities of 11.0, 14.0 and 17.5 m/s.

This indicates that in the range of velocities where PIV has been done the electric forces and the conversion of electrical to mechanical power increase with flow velocity.

So, the interaction of ions with neutral fluid particles is consequently velocity dependent, being larger when the fluid is animated with more important velocities. However, it seems that more experiments should be undertaken to confirm this tendency for a range of larger flow velocities.

Figure 7 shows the shape of the velocity profiles ratios obtained with the discharge on and off. Figures 8 show the difference of these velocities ratio profiles at different streamwise stations and for different flow velocities.

We can observe on these figures how in the field of view of our experiments the electric forces modify the velocity profile.

The magnitude of the velocity differences with discharge on and off are larger in a region about 1.5 cm measured from the plate surface. This region being more important with increasing distances from the leading edge.

We observe in Figures 8 a, b and c that the changes in the velocity field produced by the EHD actuator are more pronounced in fluid layers close to the wall. At larger distances from the leading edge, the changes tend to be more uniform and velocities differences can be detected in layers at larger wall distances.

This can be explained considering that the momentum changes on the boundary layers produce changes on the flow that are subjected simultaneously to diffusion (mainly in the direction of the normal to the surface) and convection processes (mainly in the flow direction).

At positions closer to the leading edge, streamlines far from the surface "feel" less what happens at the boundary than those quite close to it. As we consider positions at distances more important from the leading edges, diffusion modifies the momentum of the less perturbed layers (those far from the surface) and the velocity profile modifications penetrate more in the fluid .

The shapes of curves of Figure 7 are similar to the ones obtained with the OGADUP with Pitot probes placed downstream of the device [22].

Comparing EHD with OGADUP we observe that in both cases an important acceleration has been detected. However, the acceleration of the fluid layers close to the surface produced with the EHD actuator does not have the non-uniformities in the spanwise directions shown in the article above referenced.

Also, our results shows larger changes produced with the EHD device than those with the OGADUP. However a direct comparison of the performance of both actuators is not possible as the values obtained correspond to different streamwise locations.

CONCLUSIONS

We show in this article that the characteristics of a corona discharge in the proximity of extraneous bodies are quite similar if this body has a cylindrical geometry or if it is of the flat plate type. The physical phenomena involved in the description of the plasma sheet creation are similar to the ones occurring in the formation of repetitive ionization waves, like the ones appearing in streamers.

The effect of the dc corona discharge on the flow operating in the generalized glow regime is very distinctive because of two main factors :

- its intensity (luminescence in all the arc distance could be associated to ionization produced by high velocity charged particles)
- the homogeneity of the discharge occurring all along the electrode length.

From flow visualization results it can be concluded that at low Re number the effect of the discharge in the fluid dynamics close to the wall is important. However, this effect is highly dependent on the regime of discharge considered.

PIV measurements enabled us to corroborate this and to conclude that strong effects of this kind of EHD actuators on the flow are not limited to very small flow velocities as suggested by Roth in[22].

As a result, in the range of velocities considered an important effect on the control of heat transfer or in drag reduction may be expected to be attained with these actuator. Experiments considering a larger range of flow velocities and an optimization of the electrode configuration should be considered in a future work.

Acknowledgements: This research has been done with grants UBACYT AI-25 and PICT 12-02177 of the Argentine government
We would like to thank the authorities of the University of Poitiers for inviting Prof. G. Artana to the Laboratorie d'Etudes Aerodynamiques during January and February of 2000 where PIV and visualisation experiments were done.

REFERENCES

1. Loeb L., "*Electrical Coronas*", Univ. Of California Press, Berkeley, 1965, pp 552-608.
2. Goldman M., Sigmond R., "Corona and Insulation", *IEEE Trans. On El. Insul.*, Vol 17, No 2, 1982, pp 90-105.
3. Velkoff H., Godfrey R., "Low Velocity Heat Transfer to a Plate in the Presence of a Corona Discharge in Air", *J. Of Heat Transfer*, Vol 101, 1979, pp 157-163.
4. Velkoff H, Kulacki F, "Electrostatic Cooling", ASME paper No 77-DE-36, 1977
5. Kibler K., Carter G., "Electrocooling in Gases", *J. Appl. Phys,* Vol 45, 1974, pp 4436-4439.
6. Ohadi M., Li S., Dessiatoun S., "Electrostatic Heat Transfer Enhancement in a Tube Bundle Gas-to-Gas Heat Exchanger", *J. of Enhanced Heat Transfer*, Vol 1, 1994, pp 327-335.
7. Ohadi M., Nelson D., Zia S., "Heat Transfer Enhancement of Laminar and Turbulent Pipe flow via Corona Discharge", *Intnl. J. of Heat and Mass Transfer*, Vol 34, 1991, pp 1175-1187.

8. Noger C., Chang J. S., Touchard G., "Active Controls of Electrohydrodynamically Induced Secondary Flow in Corona Discharge Reactor" *Proc. 2nd Int'l Symp Plasma Techn. Polution Cont,* Bahia, 1997, pp136-141
9. Vilela Mendes R., Dente J., "Boundary Layer Control by Electric Fields", *Journal of Fluid Engineering,* Vol 120, 1998, pp 626-629.
10. El-Khabiry S., Colver G., "Drag Reduction by D.C. Corona Discharge Along an Electrically Conductive Flat Plate for Small Reynolds Number Flows", *Physics of fluids*, Vol 9, No 3, 1997, pp 587-599.
11. Colver G., El-Khabiry S., "Modeling of DC Corona Discharge Along an Electrically Conductive Flat Plate with Gas Flow*", IEEE Trans on Industry Appl.,* Vol 35, No 2, 1999, pp 387-394
12. Soetomo F., "The influence of High Voltage Discharge on Flat Plate Drag at Low Reynolds Number Air Flow", M. S. Thesis, Iowa State University, Ames, Iowa, 1992.
13. Bushnell D., "Turbulent Drag Reduction for External Flows", AIAA-83-0231, Jan. 1983.
14. Malik , Weinstein L., Hussaini M., "Ion Wind Drag Reduction", AIAA-83-0231, Jan. 1983.
15. Kallio G., Stock D., "Interaction of Electrostatics and Fluid Dynamic Fields in Wire-Plate Electrostatic Precipitators, J. Fluid Mechs, Vol 249, 1992, pp 133-166.
16. Soldati A., "Turbulence Control and Drag Reduction by Means of Large-scale Electrohydrodinamic Structures", *Proc. Intnl Workshop on Elect. Conduction, Convection & Breakdown in Fluids*, Sevilla, 1998, pp 119-125.
17. Soldati A., Banerjee S., "Turbulence Modification by Organized Electrohydrodynamic Flows", *Physics of Fluids*, Vol 10, 1998, pp 1742-1756.
18. Cahn M., Andrew G., "Electroaerodynamics in Supersonic Flow", AIAA paper No 68-24, NY, Jan. 1968.
19. Sin-I-Cheng, Goldburg A., "An analysis of the possibility of Reduction of Sonic Boom by Electroaerodynamic Devices", AIAA paper No 69-38, NY, Jan. 1969.
20. Poggie J., "Modeling the Propagation of a Shock Wave Through a Glow Discharge", *AIAA Journal,* Vol 38, No8, 2000, pp 1411-1418,.
21. Adamovich I., Subramanian V., Rich. J., Macheret S., "Phenomenological Analysis of Shock-wave Propagation in Weakly Ionized Plasmas", *AIAA Journal,* Vol, 36, No 5, 1998, pp 816-822.
22. Roth J. R., Sherman D., "Boundary Layer Flow Control with a One Atmosphere Uniform Glow Discharge Surface Plasma" , AIAA paper 98-0328, Jan. 1998.
23. Corke T., Mattalis E., "Phased Plasma Arrays for Unsteady Flow Control", AIAA paper 2000-2323, June 2000.
24. Lorber P., McCormick D., Pollack M., Breuer K., Corke T., Anderson I., "Rotorcraft Retreating Blade Stall Control", AIAA paper 2000-2475, June 2000.
25. Artana G., Desimone G., Touchard G., "Study of the Changes in the Flow Around a Cylinder Caused by Electroconvection", *Electrostatics'99*, IOP Publ. Ltd, Bristol-Philadelphia, 1999, pp 147-152.
26. Desimone G., DiPrimio G., Artana G., "Modification of the Flow Around a Cylinder by Means of Electrodes Placed on its Surface", *Proc. Colloque de la Societé Francaise d'Electrostatique*, Poitiers, June 1999, pp 80-84.
27. R. Keane, Adrian R., "Theory of Cross Correlation Analysis of PIV Images", *Applied Scientific Research*, Vol 49, 1992, pp 191-215.
28. Andreev S., Belousova I., Dashuk P., Zaroslov D., Zobov E., Karlov N., Kuz'min G., Nikiforov S., Prokhorov A., "Plasma-sheet Co_2 Laser", *Sov. J. Quantum Electron*, Vol 6, No 8, 1976, pp 931-934.
29. Dashuk P., Kulakov S., "Formation of an Electron Beam in the Plasma of a Skimming Discharge", *Sov. Tech. Phys. Lett*, Vol 7, No 11, 1981, pp 563-565.
30. Atanasov P., Grozdanov K., "Simultaneous Ultraviolet and Infrared Emission in a Sliding-Discharge Excited Laser*", IEEE J. Of Quantum Electronics*, Vol 32, No 7, 1996, pp 1122-1125.
31. Baranov V., Borisov V., Vysikailo F., Kiryukhin B., Khristoforov O., "Analysis of Sliding Discharge Formation", Kurchatov Inst. Atom. Energy, N°3472/7, (in Russian), Moscow, 1981.
32. Beverly R., "Electrical Gasdynamics and Radiative Properties of Planar Surface Discharge", *J. Appl. Phys.,* Vol 60, No1, 1986, pp 104-124.
33. Rutkevich I., "Structure of a Grazing Discharge Front", *Sov. Phys.-Tech.Phys,* Vol 31, No 7, 1986, pp. 841-842.
34. Lagarkov A., Rutkevich I., "*Ioniztion Waves in Electrical Breakdown of Gases*", Springer-Verlag, NY, 1993, pp 195-207.
35. Sigmond R., Goldman M., "Positive Streamer Propagation in Short Gaps in Ambient Air", *Proc 15th Int. Conf. On Phenomena in Ionized Gases*, Minsk, 1981, pp 649-651.
36. Seaver A., "Onset Potential for Unipolar Charge Injection", *IEEE/IAS*, Toronto, Canada, October 1993, pp 1-7.
37. Fuchs N., "*The Mechanics of Aerosols*", Dover, NY, 1964, pp 21-180.
38. Bailey A., "*Electrostatic Spraying of Liquids*", John Wiley&Sons, NY, 1988, pp 38-41.

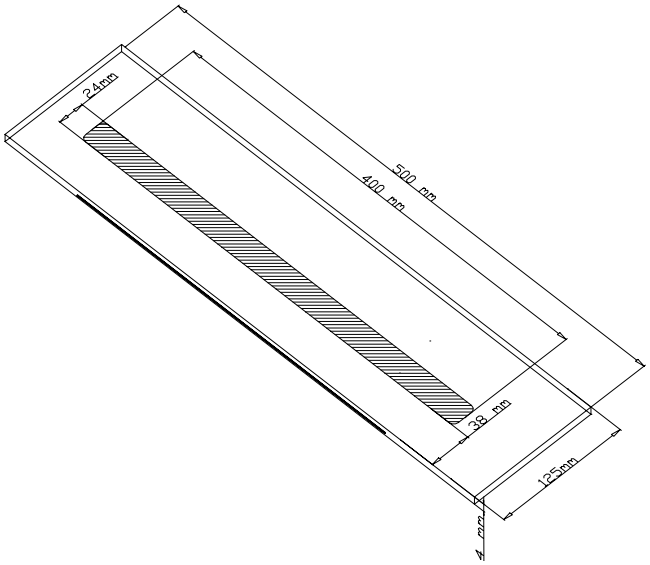

Figure 1 Plate and Electrode arrangement

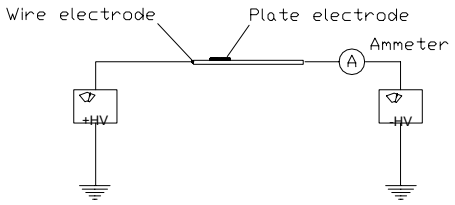

Figure 2: Schematic of the electric circuit

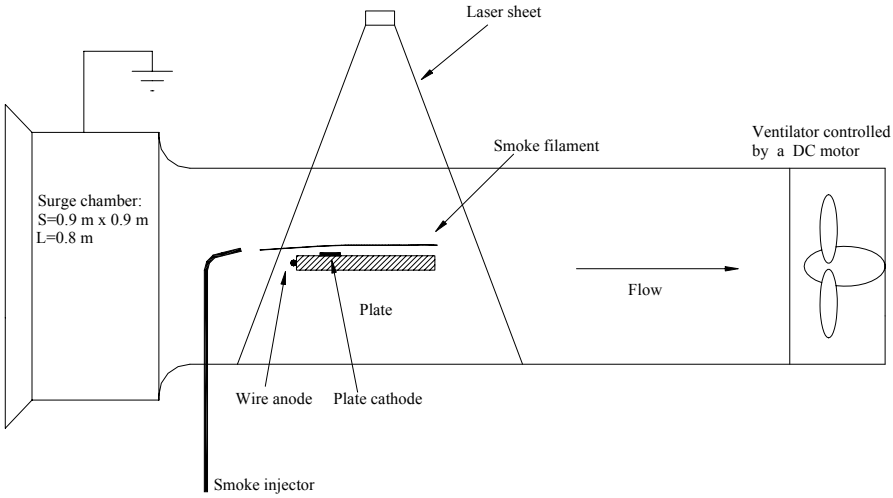

Figure 3: Schematic of the wind tunnel

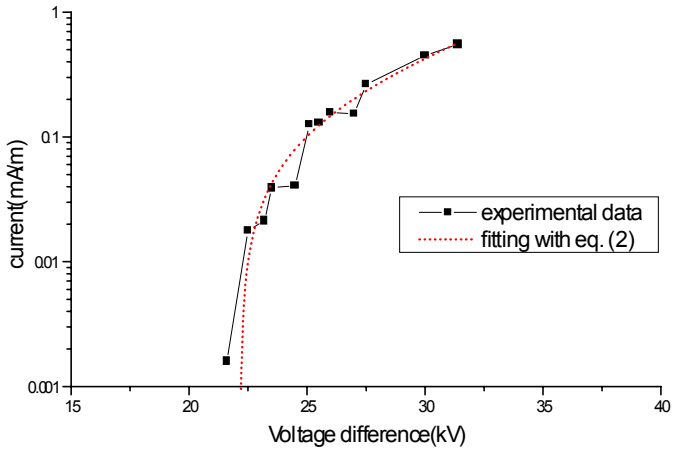

Figure 4: Voltage current curve. Electrode distance 38 mm. Electrode length 400mm

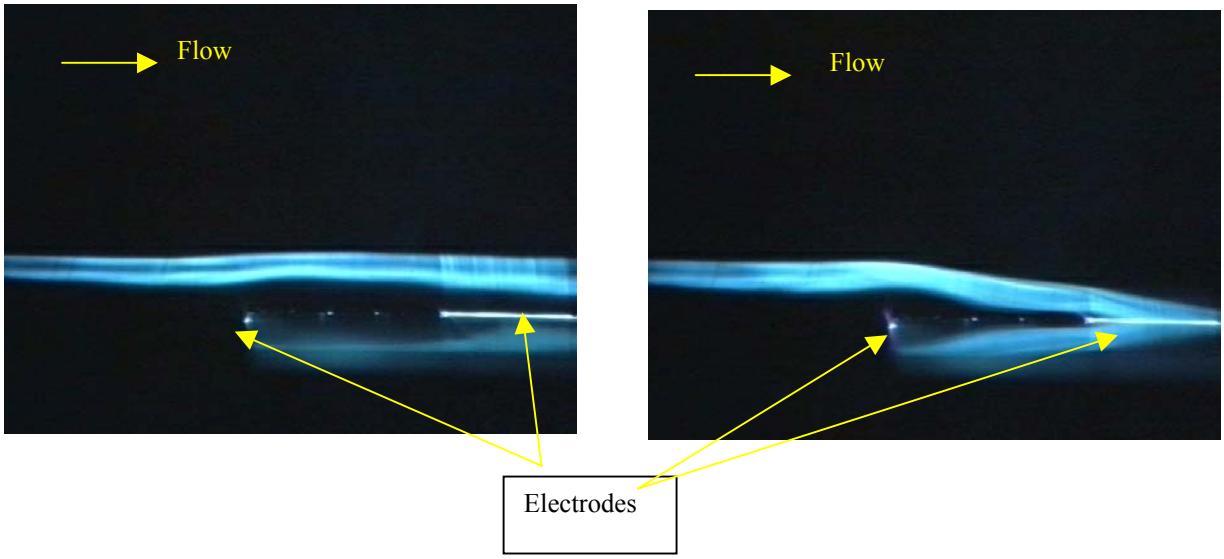

Figure 5a: Flow visualisation-Discharge off-U=0.8 m/s

Figure 5b: Flow visualisation-Discharge on-U=0.8 m/s. ΔV=33.0kV.

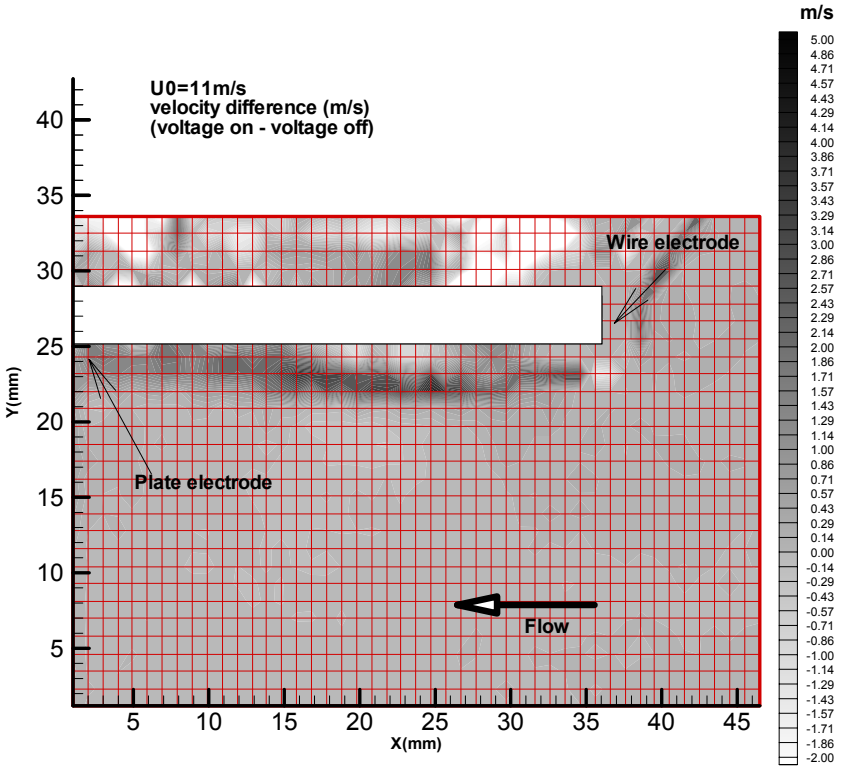

Figure 6a: Averaged velocity field differences U_0= 11.0m/s. Discharge on with ΔV=31.4 kV. Upwards illumination with the laser sheet. Above of the plate values are influenced by the shadow of the plate

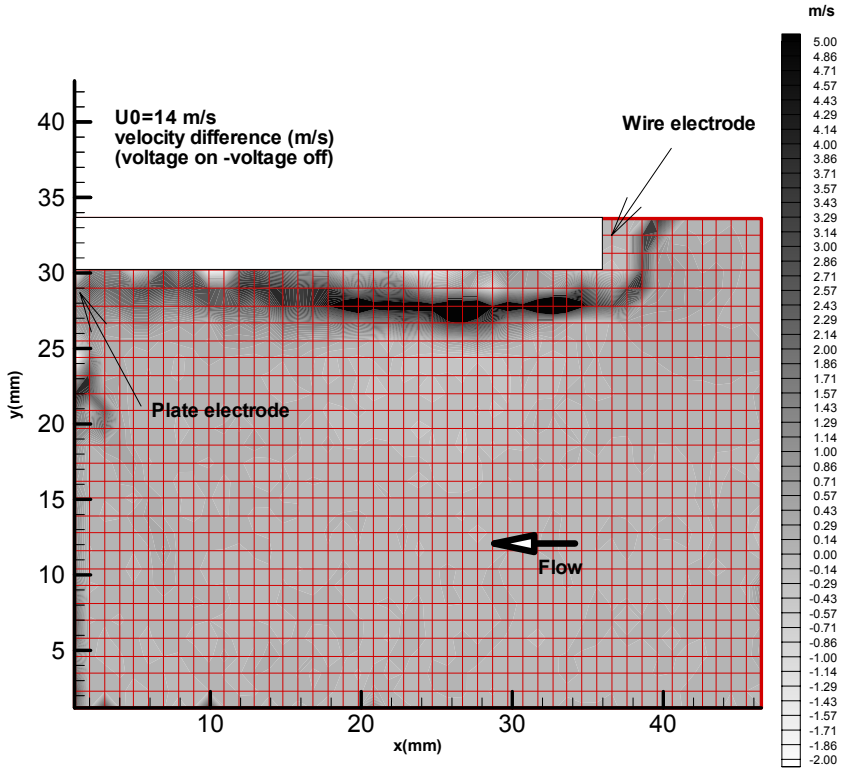

Figure 6b: Mean velocity field difference U_0=14.0m/s. Discharge on with ΔV=31.0 kV. Upwards illumination with the laser sheet.

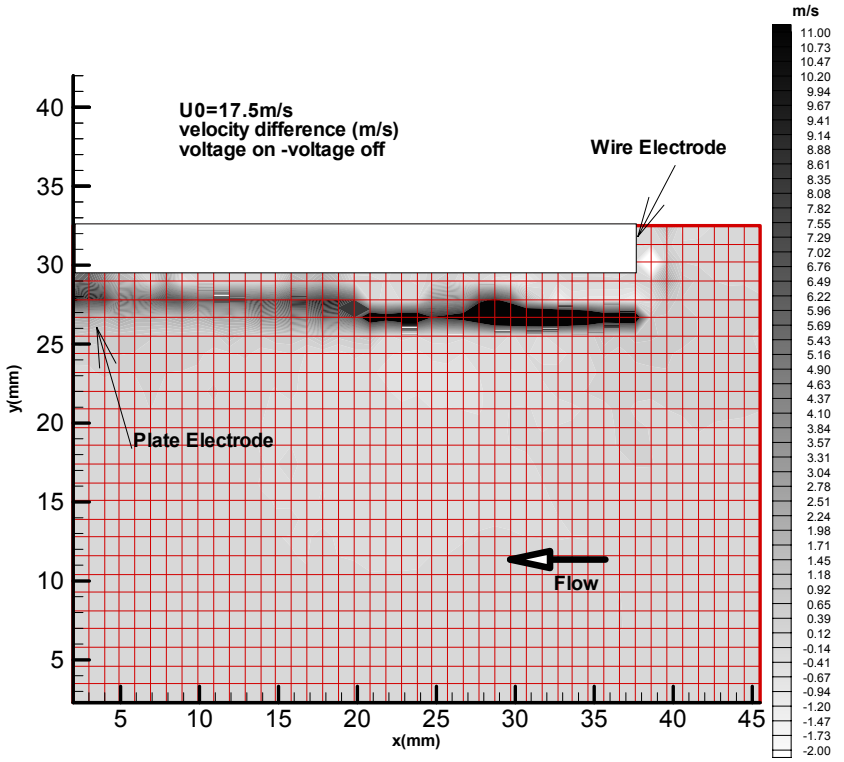

Figure 6c: Mean velocity field difference U_0=17.5m/s. Discharge on with ΔV=31.0 kV. Upwards illumination with the laser sheet.

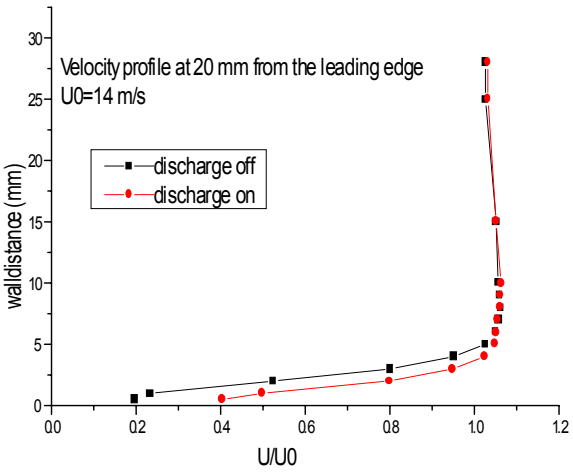

Figure 7 Typical velocity profile ratio. Streamwise station 20 mm from the leading edge. Mean flow velocity U0=14.0 m/s. Discharge voltage ΔV=31.0 kV

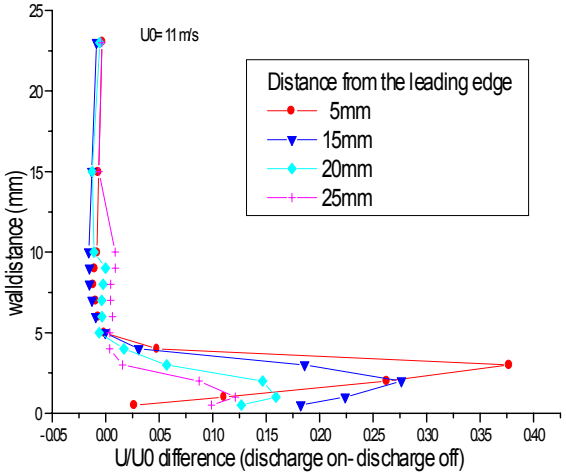

Figure 8a: Velocity difference ratio profiles at difference streamwise stations, mean flow velocity U0=11.0 m/s. Discharge voltage ΔV=31.4 kV

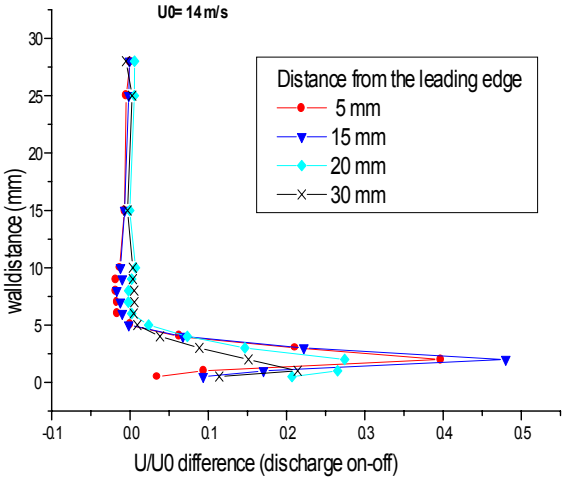

Figure 8b: Velocity difference ratio profiles at difference streamwise stations, mean flow velocity U0=14.0 m/s. Discharge voltage ΔV=31.0 kV

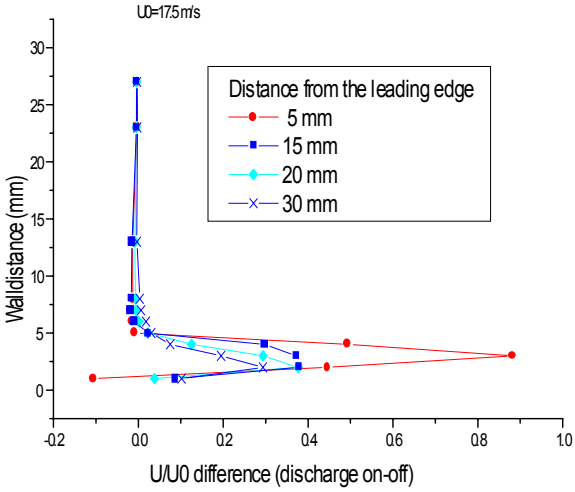

Figure 8c Velocity difference profiles, at difference streamwise stations, U0=17.5 m/s. Discharge voltage ΔV=31.0 kV